Advances in Aeronautical Science and Engineering
ISSN: 1674-8190

Mean velocity characteristics in the asymmetric far wake behind GAW (2) airfoil

N. Subaschandar*

Department of Mathematics and Statistical Sciences, Botswana International University of Science and Technology, Botswana

*Email: raos@biust.ac.bw

ABSTRACT

The two-dimensional turbulent asymmetric far wake behind a General Aviation Wing-2 cambered airfoil section is studied at a subsonic speed at zero angle of attack. The near wake flow is the region of the wake flow close to the trailing edge of the airfoil, which is dictated by the interaction of the on-coming turbulent boundary layers. Far wake is the region of the wake flow which is at a large distance from the training edge. In the current research work, mean velocity measurements have been made and analysed in the far wake, where initial asymmetric wake has become symmetric with respect to the minimum velocity line. Minimum mean velocity, wake half thickness, momentum thickness and shape parameter based on the streamwise component of mean velocity development in the turbulent asymmetric far wake are presented here. Governing equations have been solved with appropriate boundary conditions in the far wake. Self-similarity solutions have been obtained for the governing equations for mean velocity distributions. Results of self-similarity analysis have been compared with experimental data. The focus on far wake flow behaviour with mean velocity profile asymmetry, is motivated by their importance of the high-lift systems utilized in the commercial transport airplane designs.

Keywords: Far wake, GAW(2) airfoil, mean velocity, momentum thickness, drag coefficient.

1. INTRODUCTION

Turbulent wake region is the zone of fluid flow after the trailing edge of an object where the upstream turbulent boundary layers, on the upper and lower surfaces, merge into one single shear layer. The near wake is the zone of the turbulent wake fluid flow just after the trailing

edge of the body where the fluid flow is greatly influenced by the upstream fluid flow conditions and by the characteristics of the object [Townsend,1956]. It is in the wake zone that the turbulent boundary layers, separated by the upstream rigid surface, coalesce into a single free turbulent shear layer, which is not experiencing any rigid boundary conditions [Srinivasan and Narasimha,1982; Prabhu and Patel,1982; Subaschandar,2005; Subaschandar and Prabhu,1999a]. Successful estimation of the performance of objects such as airfoils, turbine and compressor blades and underwater and surface vehicles needs excellent knowledge of the fluid flow behaviour in the turbulent wake region. The evaluation and understanding of fluid flow in the turbulent wake are vital as the fluid flow in this zone is still greatly guided by the upstream trailing edge flow characteristics. Hence the study of fluid flow in this zone represents a significant aerodynamic research problem, especially connected to lift and drag and to estimate the total drag force on the body, it becomes vital to calculate the wake parameters in the far wake zone [White,2009]. Most of the investigations in the turbulent near wake, theoretical as well as experimental, are limited to the two-dimensional symmetric wake flows behind two-dimensional flat plates and airfoils at low speeds [Andreopolous and Bradshaw,1980; Chevary and Kovaznay,1969; Ramaprian et al,1982; Ramaprian et al.,1981; Subaschandar and Prabhu,1999a; Subaschandar, 2000; Alber,1980; Bogucz and Walker,1988]. On the other hand, the far wake region is at a large distance from the trailing edge where the flow is less influenced by the initial conditions at the trailing edge. The evaluation and understanding of flow in the far wake are important as the flow in this region is solely dependent on the gross parameters like total drag of the body. In this zone the fluid flow progress takes place with a sudden modification in the boundary condition. It is recognised that, even in the situation where the flow separation is non-existent, the pressure coefficient variation over the rear of streamlined objects is imposed by the collaboration between the turbulent boundary layer, the turbulent

wake flow and the external fluid flow [Narasimha and Prabhu,1972; Prabhu and Narasimha,1972].

The purpose of the current research is to examine and understand, experimentally and theoretically, the asymmetric turbulent far wake flow behind a GAW(2) airfoil section which is cambered and developing from the initial asymmetric trailing edge conditions. This kind of asymmetric flow occurs in many situations, for example, the wake flow over and behind the swept wings of airplanes and wake flows generated by the blades of rotor and turbine fans. The far wake problem studied here is one of the simplest examples of asymmetric two-dimensional turbulent far wake fluid flows. Even this simple far wake flow has not been studied widely. The present research is aimed at generating a set of data on the turbulent far wake flow behind a cambered airfoil section and to comprehend the simple asymmetric two-dimensional turbulent far wake development. The GAW(2) airfoil section which is 13.6% thickness was chosen for this research because of its strong importance in many engineering applications. The GAW(2) airfoil section profile was not changed at all to make the fluid flow less complex at the trailing edge. The GAW(2) is a cambered airfoil with an asymmetric profile so that the asymmetry existing at the trailing edge is natural, not like the experiments reported by [Ramaprian et al, 1981, 1982; Nakayama and Kreplin,1994]. Ramaprian et al, 1981,1982] altered the top surface of two-dimensional symmetric flat plate by glueing sandpaper for the entire length of the model. Nakayama and Kreplin[1994] employed a flexible flat plate to get asymmetric flow conditions at the trailing edge. Subaschandar [2016a,2025] presented results in the asymmetric turbulent near wake which was developing from the trailing edge of a cambered GAW(2) airfoil section. Subaschandar and Prabhu[1999b,2002] documented extensively the three-dimensional asymmetric turbulent near wake flow behind an infinitely swept wing with GAW(2) airfoil cross section. Our emphasis in the current study was on the far wake flow region beyond a distance of about 300 trailing edge momentum thicknesses downstream of the trailing edge.

The measurements were performed in the asymmetric turbulent far wake behind a GAW(2) airfoil cross section at zero angle of attack. The airfoil is cambered with the turbulent boundary layers on the upper and lower surfaces develop under diverse streamwise pressure gradients and are attached at the trailing edge. The present study would, it is expected, give further push to study more complex asymmetric turbulent far wake flows which frequently occur in engineering applications. The asymmetric far wake flow studied here, being two-dimensional and yet relatively simple, is anticipated to provide a wide understanding of asymmetric far-wake fluid flow features and offer a good and detailed test of the capabilities of various turbulence models, numerical schemes and computational codes which take into account the asymmetry of the fluid flow. Many details regarding the experimental setup and initial conditions were described in [Subaschandar, 2016a, b, 2025] and several results were presented in the conference paper by the author of this current manuscript [Subaschandar,2016b].

The aim of the present study is to analyse and understand far wake flow developing from initial asymmetric trailing edge conditions. Many of the studies carried out in the past were concentrated in the symmetric far wake flows [Pot, 1979; Narasimha and Prabhu, 1972; Prabhu and Narasimha, 1972; Sreenivasan and Narasimha, 1982]. Self-similarity solutions have been obtained in the symmetric far wake in such flows. The far wake flow, which is developing from initial asymmetric conditions at the trailing edge, has not been studied well. The present research was started with an aim to describe far wake, with initial asymmetric conditions, in terms of self-similarity solutions for governing equations. The three-dimensional asymmetric turbulent near wake behind a swept wing with GAW(2) airfoil cross section has been studied extensively [Subaschandar and Prabhu, 2002]. Their studies showed that the turbulent wake which was asymmetric near the trailing edge exhibited symmetry by about a distance of 60 trailing edge momentum thicknesses downstream of the trailing edge [Subaschandar and Prabhu,2002]. With this in mind, our focus was concentrated in the wake region beyond a

distance of 300 trailing edge momentum thicknesses downstream of the trailing edge so that symmetry has been reached in the region of our interest.

2. EXPERIMENTAL SETUP

The experiments were performed in the 300x1500mm boundary layer wind tunnel of the National Aerospace Laboratories, Bangalore. The GAW(2) airfoil model, with a chord length(C) of 600mm and a span of 300mm, was fixed vertically in the wind tunnel test section. The airfoil model has a profile thickness of 13.6%. The measurements were conducted at an undisturbed freestream velocity of 30m/s, giving a Reynold number, based on chord length and undisturbed freestream velocity, of $1x10^6$. The measurements were performed at zero angle of incidence. The GAW(2) airfoil is a cambered airfoil and it was not modified at all to avoid fluid flow complications close to the trailing edge. The airfoil model was facilitated with 48 static pressure taps of outer diameter 1.2 mm each on both top and the bottom surfaces along the midspan in the direction of the freestream. The boundary layers on the top and bottom surfaces of the airfoil model were tripped at 10% chord from the leading-edge using transition trips (sandpaper of width 15 mm and grade 50). The sandpaper width, grade and location were chosen to give a fully developed turbulent boundary layer, at the top and bottom surfaces, at the trailing edge of the airfoil model. End plates have been employed at a distance of 10mm from the wind tunnel walls at both ends of the model for attaining the spanwise invariance. Profiles of the magnitude of the local mean velocity vector were measured by employing a pitot probe with a hole radius (outer) of 0.5 mm, along with the static pressure measured in the undisturbed freestream outside the wake. It was noticed that the total pressure measured by the pitot probe was insensitive to the probe inclination up to $\pm 4^0$. Mean velocity measurements were performed out in the wake up to a distance in the range of 1-800 trailing edge momentum thicknesses from the trailing edge. Figure 1 shows the schematic of the experimental setup used to make measurements. Figure 1 displays, also, the coordinate system employed and the mean

velocity components. Z-axis, which is not shown in the Fig.1 was perpendicular to the plane of the paper.

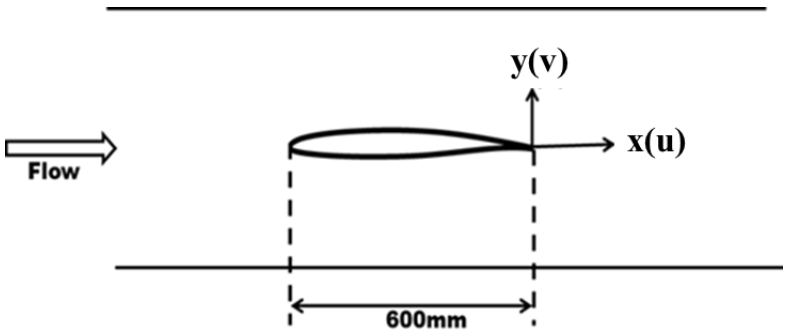

Figure 1: Schematic of the experimental setup (not drawn to scale)

3. INITIAL CONDITIONS

The development of wake flow behind any streamlined object depends on the upstream initial conditions of the fluid flow at the trailing edge of the model. The values of displacement thickness, momentum thickness and shape factor for both upper and lower surfaces of the airfoil model at a location just upstream of the trailing edge of the geometry are given in the Table 1. The integral parameters are calculated based on the streamwise component of mean velocity. The values of integral parameters on the upper and lower surfaces show the presence of strong asymmetry at the trailing edge.

Table 1: Integral parameters at the trailing edge

Parameters →	δ*(mm)	θ(mm)	H
Top surface	3.6	2.1	1.534
Bottom surface	0.8	0.5	1.416

Reynolds numbers calculated using total displacement thickness and total momentum thickness near the trailing edge, are about 8700 and 5200 respectively. Although the displacement thickness and momentum thickness Reynolds numbers are not very high, they can be considered to be high enough to provide results independent of Reynolds numbers. Total drag was

computed from pitot-static measurements in the far wake by using the method of [Jones,1936] as described in [Dos Santos et al, 2006; Schlichting, 1979] at three streamwise locations (namely, x/C=1.5, 1.75 and 2.0). The total drag coefficient at these three streamwise locations were plotted and shown in the Fig. 2. The graph shows very little difference in the values of total drag coefficients at these three streamwise locations confirming the presence of two-dimensionality in the flow. The mean velocity measurements were carried out in the three horizontal planes along the span (Z-direction) of the model close to the trailing edge (namely, Z=-75mm, Z=75mm and Z=0mm.) and are presented in the Fig. 3. A very good agreement was seen among the measurements at the three spanwise locations confirming the presence of spanwise invariance of mean velocity profiles.

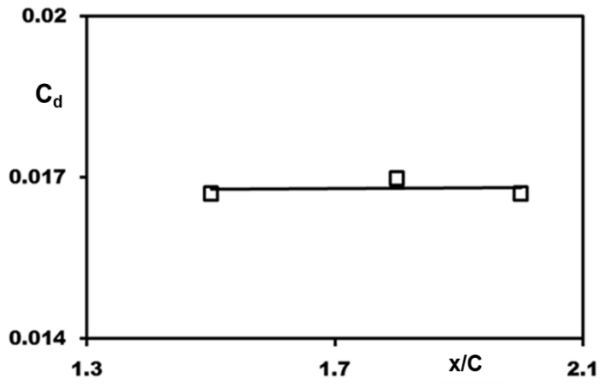

Figure 2: Total drag coefficient calculated using wake survey method at three locations

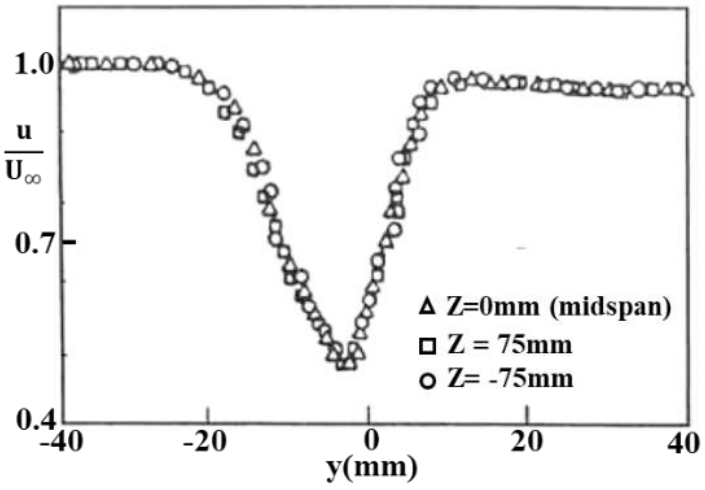

Figure 3: Streamwise component of mean velocity profiles at the three locations along the span of the model close to the trailing edge.

Figure 4 presents the static pressure coefficient profile on the cambered airfoil along the chord length. The static pressure coefficient distribution shows that the turbulent boundary layer is only under a moderate adverse streamwise pressure gradient and the fluid flow is attached at the trailing edge of the model. These remarks are reinforced by the fact that the shape factor has a value of about 1.5 at the trailing edge.

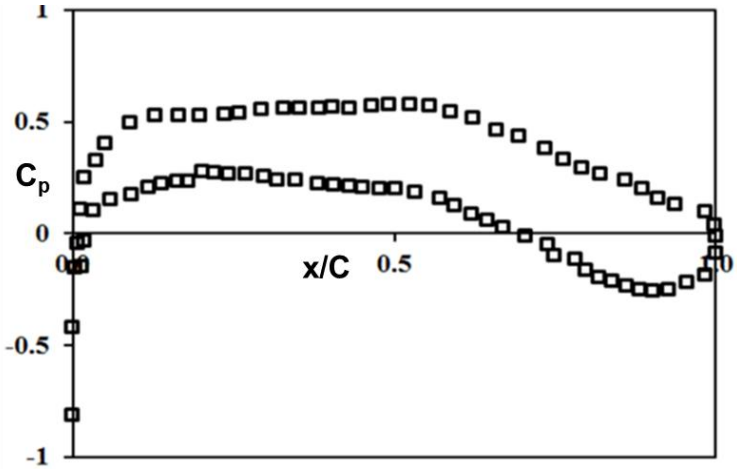

Figure 4: Static pressure coefficient distribution on the airfoil model

With these initial conditions on the model and at the trailing edge, the development of far wake flow is analysed in the next sections.

4. SIMILARITY ANALYSIS

In this section, an attempt is made to extend the self- similarity analysis which is valid for symmetric two- dimensional far wake to the far wake flow evolving from initial asymmetric trailing edge conditions. Far wake flow is analysed using continuity and momentum equations. Most of the analysis follows the steps of two-dimensional far wake analysis given in [Ramaprian et al, 1981; Subaschandar, 2016b]. With the notations shown in the Fig. 1, the governing equations for the far wake flow are

$$\frac{\partial u}{\partial x} + \frac{\partial v}{\partial y} = 0. \tag{1}$$

$$u\frac{\partial u}{\partial x} + v\frac{\partial u}{\partial y} = \frac{1}{\rho}\frac{\partial \tau}{\partial y} \quad . \tag{2}$$

The freestream velocity outside the wake is assumed to be constant(U_∞) and $\boldsymbol{\tau = \mu\frac{\partial u}{\partial y} - \rho\overline{u'v'}}$ is the total shear stress. We seek a similarity solution of the form

$$\boldsymbol{\tau = \rho W_0^2 g(\eta),\ W = W_0 f(\eta).} \tag{3}$$

where $\mathbf{W = (U_\infty - u)}$ is the velocity defect and $\boldsymbol{\eta = \frac{y}{B}}$. W_0 (maximum velocity defect at the minimum mean velocity line in the wake) and B (wake half-thickness) are the local velocity and length scales, respectively. With these substitutions, Eqs (1) and (2) reduce to

$$\left[\frac{U_\infty B'}{W_0} - \underline{B'f}\right]\eta f' - \left[\frac{U_\infty W_0'}{W_0^2}B - \underline{\frac{W_0'B}{W_0}f}\right]f - f'\underline{\int\left\{\frac{W_0'B}{W_0}f - B'\eta f'\right\}d\eta} - g' = 0. \tag{4}$$

At large distances from the body, the mean velocity defect is small, i.e $\mathbf{W_0 << U_\infty}$, and the underscored terms in the Eq. (4) are of second order or smaller. Hence

$$\frac{(U_\infty B)'}{W_0}\eta f' - \frac{B(U_\infty W_0)'}{W_0^2}f - g' = 0. \tag{5}$$

If this asymptotic wake is self-preserving, then the Eq. (5) leads to the following well-known result for a far wake with a nonzero momentum thickness [Ramaprian et al, 1981; Townsend,1956; Schlishting,1979]

$$B \sim x^{1/2} \quad \text{and} \quad W_0 \sim x^{-1/2}. \tag{6}$$

These half-power growth and decay laws can therefore be used to measure the approach of the mean flow to asymptotic conditions.

In order to evaluate the constants in the Eq. (6) and determine the mean velocity profile f(η), it is necessary to invoke a turbulence closure model. Therefore, for example, introduction of a constant eddy-viscosity, ν_τ, viz

$$\frac{\tau}{\rho} = \nu_\tau\frac{\partial u}{\partial y} = \nu_\tau\frac{W_0}{B}f' = g = -\frac{\nu_\tau}{W_0 B}f'.$$

reduces Eq. 5 to

$$\frac{\nu_\tau}{W_0 B}f'' + \left(\frac{U_\infty B'}{W_0}\right)\eta f' - \left(\frac{U_\infty B W_0'}{W_0^2}\right)f = 0. \tag{7}$$

which is identical with that for laminar flow except that ν(molecular viscosity) has to be replaced by ν_T (turbulent eddy viscosity) [Schlichting, 1979]. With the appropriate boundary conditions, the solution of the Eq. (7) is

$$f = \frac{W}{W_0} = \exp(-4\eta^2 \ln 2). \tag{8}$$

$$B = 4\sqrt{\ln 2}\left(\frac{\nu_\tau x}{U_\infty}\right)^{1/2}. \tag{9}$$

$$\frac{W_0}{U_\infty} = \frac{1}{\sqrt{\pi}}\left(\frac{U_\infty C_d d}{\nu_\tau}\right)^{1/2}\left(\frac{C_d d}{x}\right)^{1/2}. \tag{10}$$

where $C_d = \frac{D}{\left(\frac{1}{2}\right)\rho U_\infty^2 d}$ is the drag coefficient, D is the total drag force and d is the characteristic length of the body. The overall momentum shows that $C_d d = 2\theta$ where

$$\theta = \int_{-\infty}^{\infty} \frac{u}{U_\infty}\left(1 - \frac{u}{U_\infty}\right) dy.$$

is the constant, asymptotic momentum thickness of the far wake. Using θ as a length scale, the Eqs. (9) and (10) become

$$\left(\frac{B}{\theta}\right)^2 = 16\left(\frac{\nu_\tau}{U_\infty \theta}\right)\left(\frac{x}{\theta}\right)\ln 2. \tag{11}$$

$$\left(\frac{U_\infty}{W_0}\right)^2 = 4\pi\left(\frac{\nu_\tau}{U_\infty \theta}\right)\left(\frac{x}{\theta}\right). \tag{12}$$

From an examination of some early results from the far wake of cylinders, Schlichting [1979] deduced a value of 0.0444 for $\left(\frac{\nu_\tau}{U_\infty \theta}\right)$. However, Townsend [1956] quotes a value of 0.032, which is identical with the average value deduced from the asymptotic turbulent far wake data [Narasimha and Prabhu, 1972]. A value of 0.032 was found to be suitable in the present analysis also. It should be noted that the constants in the above results are derived based on a constant eddy-viscosity model, which is not entirely realistic in view of the marked intermittency of the flow over a large part of the wake region.

5. RESULTS AND DISCUSSION

In this section, results of the above analysis are compared with the experimental data obtained in the asymmetric far wake behind a GAW(2) airfoil. The appropriate value of $\boldsymbol{\theta}$ was determined from the data of the most downstream station to avoid any uncertainties occurring from the measurements near the trailing edge. Figure 5 shows measured mean velocity profiles in the far wake flow at several streamwise stations. Since it was observed that the mean velocity profiles had reached symmetry only one half of the profiles are shown in the Figure 5. Also, shown in the Figure 5, is the self-similar exponential curve given in the Eq. (8). It can be seen from the Figure 5 that the measured data are in good agreement with the exponential asymptotic profile except for some small departures near the outer edge of the wake.

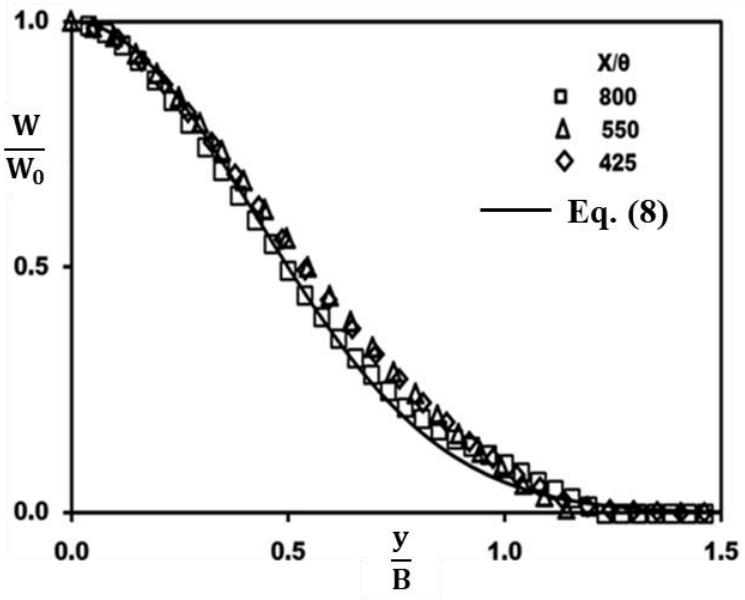

Figure 5: Mean velocity profiles in similarity variables in the far wake

Figure 6 shows the variation of wake half thickness in the asymmetric turbulent far wake. The Fig. 6, also, shows the relationship for wake half thickness as given by the Eq. (11) with $\frac{\nu_\tau}{U_\infty \theta} = 0.032$. From the Fig. 6 it is clearly seen that the wake half thickness does not follow the asymptotic power laws with the prescribed constant value of eddy-viscosity until about x/θ =

300 and after that the agreement between the measured data and the analytical results is reasonably good.

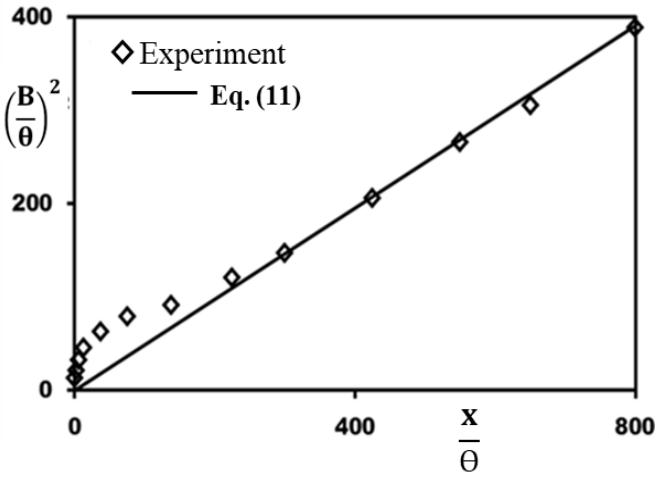

Figure 6: Streamwise development of wake half-thickness in the far wake

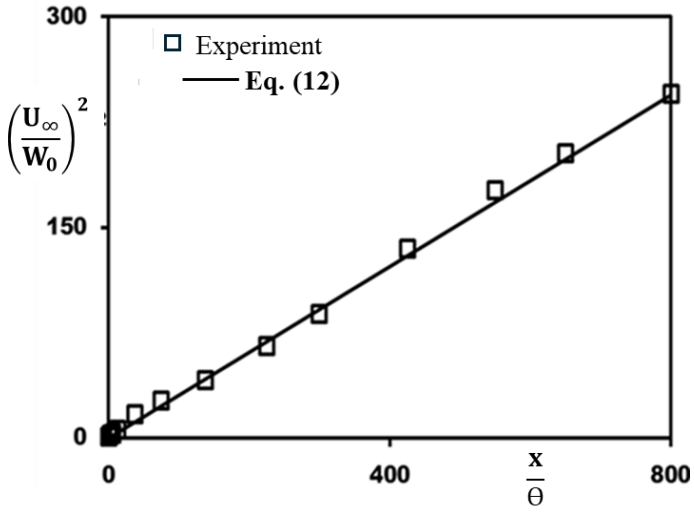

Figure 7: Streamwise development of inverse of maximum velocity defect in the far wake

Figure 7 shows the variation of inverse of maximum velocity defect in the turbulent far wake. The Fig. 7 also shows the relationship for inverse of maximum velocity defect as given by the Eq. (12) with $\frac{\nu_\tau}{U_\infty \theta} = 0.032$. From this figure it is clearly seen that the inverse of the maximum velocity defect does not follow the asymptotic power law with the prescribed constant value of eddy-viscosity until about x/θ = 300 and after that the agreement between the measured data and the analytical results is reasonably good.

In summary, the experimental data in the turbulent wake behind a GAW(2) airfoil indicate that the velocity profiles have become symmetric in the far wake. The experimental data in the turbulent far wake behind the GAW(2) airfoil indicate that the wake becomes independent of the initial conditions and approaches as asymptotic state in mean velocity at around $x/\theta = 300$.

6. CONCLUSIONS

Mean velocity measurements have been carried out in the turbulent asymmetric far wake flow region behind a GAW(2) airfoil at low speeds at zero angle of attack. Profiles of mean velocity which exhibit asymmetry close to the trailing edge, show symmetrisation around a large distance of more than 300 trailing edge momentum thicknesses. It is shown that the self-similarity analysis of a symmetric two-dimensional far wake flow can be extended to the far wake flow of an initially asymmetric wake flow. The results of self-similarity analysis agree well with experimentally measured mean velocity data in the far wake. The wake half-thickness and inverse of maximum velocity defect from the self-similarity analysis agree well with the experimental data in the far wake and are shown to follow the half power laws derived in the self-similarity analysis. The results presented in this paper not only would be useful to validate various turbulence models, numerical schemes and computational codes, but also, provide impetus to research on more complex asymmetric far wake flows developing from initial asymmetric conditions.

Acknowledgements

Author acknowledges the support received from the Department of Mathematics and computational Sciences and BIUST authorities in carrying out this research.

FUNDING SOURCES

This research study did not receive any specific grant from funding agencies in the public, commercial, private, or not-for-profit sectors.

DECLARATION OF COMPETING INTEREST

The author declares that he does not have any competing financial interests or personal relationships that could appear to influence the work reported in this paper.

REFERENCES

[1]. Townsend, A.A. (1956). The Structure of Turbulent Shear Flow. Cambridge University Press, Cambridge, UK.

[2]. Sreenivasan, K. R. and Narasimha, R. (1982). Equilibrium Parameters for Two-Dimensional Turbulent Wakes. ASME Journal of Fluids Engineering, 104(2), pp. 167–169. https://doi.org/10.1115/1.3241801.

[3]. Prabhu, A. and Patel, V.C. (1982). Analysis of turbulent near wakes, IIHR Report No. 253, University of lowa, U.S.A.

[4]. Subaschandar, N. (2005). Measurements in the Turbulent Near-wake Behind an infinitely swept Flat Plate. Journal of Experimental Thermal and Fluid Science, 29(4), pp. 415-423. https://doi.org/10.1016/j.expthermflusci.2004.04.003.

[5]. Subaschandar, N. and Prabhu, A. (1999a). Turbulent near-wake development behind a flat plate. Journal of Aerospace Science and Technology, 1(2), pp. 61–70. https://doi.org/10.1016/ S1270-9638(99)80030-3.

[6]. White, F.M. (2009). Viscous Fluid Flow. 7th Edition, McGraw-Hill, McGraw-Hill Companies, Inc., New York, USA. www.mhhc.com. ISBN 978–0–07–352934–9.

[7]. Andreopoulos, J. and Bradshaw, P. (1980). Measurements of interacting turbulent shear layers in the near wake of a flat plate. Journal of Fluid Mechanics, 100(3), pp. 639–668. https:// doi.org/10.1017/S0022112080001322.

[8]. Chevray, R. and Kovasznay, L. S. G. (1969). Turbulence measurements in the wake of a thin flat plate. AIAA Journal, 7(8), pp. 1641–1643. https://doi.org/10.2514/3.5461.

[9]. Ramaprian, B. R., Patel, V. C. and Sastry, M. S. (1982). The symmetric turbulent wake of a flat plate. AIAA Journal, 20(9), pp. 1228–1235. https://doi.org/10.2514/3.7972.

[10]. Ramaprian, B. R., Patel, V. C. and Sastry, M. S. (1981). Turbulent Wake Development behind Streamlined Bodies. Iowa Institute of Hydraulic Research Report 231, University of Iowa, USA.

[11]. Subaschandar, N. (2000). Prediction of turbulent near and far wake flows using four turbulence models. Computational Fluid Dynamics Journal, 8, pp. 544-560. https://ci.niiac.jp/ ncid /AA10930387?l=en#anc-resource.

[12]. Alber, I. E. (1980). Turbulent Wake of a Thin Flat Plate. AIAA Journal, 18(9), 1044–1051. https://doi.org/10.2514/3.50853.

[13]. Bogucz, E.A. and Walker, J.D.A. (1988). The turbulent near wake at a sharp trailing edge. Journal of Fluid Mechanics, 196, pp. 555–584. http://doi.org/10.1017/S002211208800 2812.

[14]. Narasimha, R. and Prabhu, A. (1972). Equilibrium and relaxation in turbulent wakes. Journal of Fluid Mechanics, 54(1), pp. 1–17. https:/doi.org/10.1017/S0022112072000 497.

[15]. Prabhu, A. and Narasimha, R. (1972). Turbulent non-equlibrium wakes. Journal of Fluid Mechanics, 54(1), pp. 19–38. https:/doi.org/10.1017/S0022112072000503.

[16]. Nakayama, A. and Kreplin, H.P. (1994). Characteristics of asymmetric turbulent near wakes. Physics of Fluids, 6(7), pp. 2430-2439. https://doi.org/10.1063/1.868190.

[17]. Subaschandar, N. and Prabhu, A. (1999b). Turbulent near wake behind an infinitely swept wing. 8th Asian Congress of Fluid Mechanics, Shenzhen, CHINA, Dec 6-10, 1999.

[18]. Subaschandar, N. and Prabhu, A. (2002). Turbulent Near-Wake Studies Behind an Infinitely Swept Wing. Journal of Aircraft, 39(2), pp. 290–295. https://doi.org/10.2514/2.2926.

[19]. Subaschandar, N. (2016a). Mean Velocity in the Asymmetric near Wake Behind a GAW(2) Airfoil. MATEC Web of Conferences 54, 11002. https://doi.org/10.1051/matecconf/ 20165411002.

[20]. Subaschandar, N. (2016b). Mean Velocity in the Asymmetric Far Wake Behind a GAW(2) Airfoil. MATEC Web of Conferences 54, 11003. https://doi.org/10.1051/matecconf/2016541 1003.

[21]. Subaschandar, N. (2025). Mean Velocity Development in the asymmetric near wake behind a GAW(2) airfoil. Advances in Aeronautical Science and Engineering, 16(10), pp. 1-13. https:// doi.org/10.5281/zenodo.17421571.

[22]. Pot, P.J. (1979). NLR TR 79063. National Aerospace Laboratory NLR, Netherlands.

[23]. Jones, B.M. (1936). The Measurement of Profile Drag by the Pitot-Traverse Method. ARC Reports and Memoranda No. 1688, Teddington, UK.

[24]. Dos Santos, L.A., Avelar, A.C., Chiseaki, M. and Mello, O.A.F. (2006). Drag estimation by wake survey performed measuring velocities and measuring total and static pressures. Proceedings of the 11th Brazilian Congress of Thermal Sciences and Engineering-ENCIT 2006, Curitiba, Brazil, Dec. 05-08.